


**Blue, Robert and Uttamchandani, Deepak (2015) Recent advances in optical fiber devices for microfluidics integration. Journal of Biophotonics. ISSN 1864-063X , http://dx.doi.org/10.1002/jbio.201500170**

# Recent advances in optical fiber devices for microfluidics integration

R. Blue and D. Uttamchandani

**Abstract — This paper examines the recent emergence of miniaturized optical fiber based sensing and actuating devices that have been successfully integrated into fluidic microchannels that are part of microfluidic and lab-on-chip systems. Fluidic microsystems possess the advantages of reduced sample volumes, faster and more sensitive biological assays, multi-sample and parallel analysis, and are seen as the de facto bioanalytical platform of the future. This paper considers the cases where the optical fiber is not merely used as a simple light guide delivering light across a microchannel, but where the fiber itself is engineered to create a new sensor or tool for use within the environment of the fluidic microchannel.**

**Key words: optical fiber sensors, fluidic microchannels, optical trapping, microfluidics, lab-on-chip**

## I. Introduction

THE integration of microfluidics and photonic technologies onto a common physical platform has come to be known as optofluidics [1]. An emerging area of optofluidics research is the integration of fiber optic technology with fluidic microchannel platforms in order to create fluidic microsystems with new or enhanced capabilities. Microsystems themselves are miniaturized versions of common laboratory, scientific, industrial and consumer equipment that perform specific functions which include sensing or actuation steps. They are designed to gain performance advantages by operating at significantly smaller dimensions compared to traditional systems. A key element of microfluidics is the ubiquitous microchannel, which is a fluid guiding channel with lateral dimensions of the order of a few tens to a few hundreds of micrometers [2]. Fluids flowing in the microchannels may be pure or they may be transporting biological, chemical or pharmaceutical materials and compounds. Traditional procedures and apparatus for manipulating liquids in laboratories have been steadily moving to miniature platforms incorporating microfluidic elements, microsensors and microactuators. The phrase "lab-on-a-chip" is often used to describe this rapidly evolving technology. The smaller liquid volumes needed with these miniaturized systems reduces the consumption of expensive reagents and significantly lowers the cost of an assay or chemical reaction which, together with the advent of microfluidic chips fabricated from low cost polymers, has created the freedom to conduct multiple parallel biological or chemical reactions, thus accelerating measurement and research outcomes [3, 4]. The signature of many of these reactions is linked to optics and photonics, for example via light absorption, light generation, optical wavelength changes or refractive index changes. These signatures constitute "optical signals".

As volumes shrink so does the magnitude of the optical signals generated from assays or reactions. More sensitive methods and tools for measuring these low-magnitude optical signals are required. In recent years the interest in exploiting the properties and dimensions of optical fibers as high-sensitivity sensors and manipulating tools for use within the generic microchannel has grown. To date, the majority of cases where fiber optics are integrated with microfluidic channels have used the fiber optics merely as simple light guides whereby two fibers are located on opposite side walls of the microchannel and no modification of the optical fibers themselves has taken place [5-8]. The above methodology is outside the scope of this paper. Instead, this paper, examines the more innovative technologies where the optical fiber is modified to create a new sensing device or a manipulation tool that is located within the microchannel itself. This is anticipated to be of greater significance because the microchannel will become an important component of the laboratory of the future, and new methods of reproducing laboratory equipment and measurements at this scale and in this fluidic environment will be required.

Standard optical fiber consists of a 9 to 60 µm diameter core surrounded by a lower refractive index 125 µm diameter cladding , which is compatible with the transverse dimensions of microfluidic channels, and this cladding diameter is often further reduced when fabricating the fiber sensor or tool. In addition, a standard optical fiber is manufactured from silica, which offers advantages of being lightweight and chemically inert within the microchannel. In a conventional optical fiber, light energy is guided by the silica core, and the optical energy propagates by total internal reflection at the core-cladding boundary. A portion of the optical field, called the evanescent field, decays into the cladding over a distance of a few hundred nanometers. If the cladding thickness is substantially reduced, the evanescent field of the optical waveguide mode can be accessed to facilitate optical sensing. Alternatively, the light emerging from the distal end of the fiber can also be employed for optical sensing. Properties of the light that can be changed are wavelength, phase, polarization and intensity. Additionally, the optical power transported by an optical fiber can be directed into a microchannel and be used as an energy source to manipulate material within the channel.

Section II of this paper highlights that the introduction of an optical fiber system within a fluidic microchannel can result in

Manuscript received June 3rd, 2015.
R. Blue and D. Uttamchandani are with the Centre for Microsystems and Photonics, University of Strathclyde, Glasgow, Scotland, UK. (corresponding author email: d.uttamchandani@strath.ac.uk).

both faster and more senstive assays, and the arrangement can be configured for label-free sensing that can additionally lead to cost reductions. Section III shows that the optical fiber within the microchannel can match and outperform traditional bulk refractometers, while section IV demonstrates that spectroscopic identification of molecules within the microchannel can also be achieved. Section V illustrates that the optical fiber can also make rheologic measurements on the fluid itself. Finally, section VI reveals that the optical fiber additionally has the versatility to be used as a tool for the sorting and trapping of particles within the microchannel.

## II. OPTICAL FIBER MEDIATED IMMUNOASSAYS IN MICROCHANNELS

Immunoassays are used to investigate the nature of binding interactions between biological molecules, and as a method of characterization or concentration measurements [9]. Immunoassays have traditionally been conducted in multi-well plates with typical times in excess of 30 minutes for each assay incubation stage. Protein assays normally conducted in multi-well plates are being transferred to microfluidic devices [10] contributing to the potential for point-of-care diagnostics and treatment [11].

### A. Tapered optical fibers for rapid and ultrasensitive assays in microchannels

Faster assay times are important for rapid diagnosis of, for example, an acute myocardial infarction through the detection of elevated levels of cardiac biomarkers [12, 13]. Typically, clinically relevant biomarkers are isolated and tested in an in-vitro setting, often requiring a laboratory, but in recent years there has been an increasing push towards point-of-care testing, which can reduce the burden on health services.

The inherent features of the microchannel environment, namely smaller volume and flowing liquids, can lead to potentially faster assay times. For a multi-well plate with capture antibodies bound to the surface, the binding kinetics of antigens in the static bulk solution is diffusion limited, whereas in a microchannel with dynamic fluid flow the binding process is more rapid due to the fluid flow actively transporting the antigens to the capture antibodies. This is especially relevant when attempting to detect low concentrations of target molecules.

The silica cladding of an optical fiber can be reduced by polishing one side of the fiber or by tapering the full cross-section of the fiber. A tapered fiber with a waist diameter of 5 μm was experimentally shown to have approximately 14 times higher sensitivity for refractive index sensing compared to a polished fiber of equivalent length [14]. Kai et al. [15] in 2007 designed an optical fiber sensor within a microchannel by functionalizing a tapered fiber with protein receptor molecules. The optical evanescent field interacted with secondary captured antibodies labelled with a fluorophore to generate a measureable signal which was also captured by the optical fiber. The simultaneous measurement of four cardiac markers in a blood sample was achieved in less than 10 minutes. However, the optical fiber with a waist diameter of several micron results in a fragile structure that requires careful handling. In addition, optical fiber tapers are usually manufactured by expensive fabrication facilities e.g. using $CO_2$ lasers to heat and pull the fiber, or by immersion in aggressive chemicals such as buffered HF acid.

Notwithstanding these issues, the motivation for researchers to experiment and explore the possibilities of optical fiber tapers is their significantly higher sensitivity that can be attained. This was further demonstrated by Zhang et al. [16] who reduced the fiber taper diameter down to 900 nm, and over an extended length of up to 2.5 cm (with a total sensor insertion loss of only 3 dB). Such nano-diameter fibers had significantly larger optical mode field penetrating into the external medium over this extended length. These sensors were used for simple fiber absorbance measurements in a microchannel and measured the dye methylene blue to a concentration of 50 pM. This was estimated to be 2000 times more sensitive than an equivalent experiment using a 1 cm cuvette in a standard bulk spectrometer, while the sample volume used in the microchannel was only 500 nL. Subsequently, the fiber sensor was applied to a biological assay of labelled bovine serum albumin in the microchannel (Figure 1), and indicated a limit of detection close to 10 fg/mL, which, as noted by the authors, is orders of magnitude greater than using traditional assay methods. The fact that silica fibers could be thinned to such small transverse dimensions and incorporated into a microchannel to create a sensor demonstrated that fragility should not be a barrier for investigating future sensors for ultra-sensitive analysis within fluidic microsystems. In fact, optical fibers at these nano dimensions acquire an increased flexibility (compared to micro-diameter fibers) that allows them to move freely and even be tied into knots [17]. Additionally, in comparison to related sensors of these dimensions, such as a semiconductor nanowires interrogated by a photoluminescence system [18] or single polymer nanowire sensors addressed by optical tapers [19], the sensor is also more compact and is easier to address via standard optical fiber connectors.

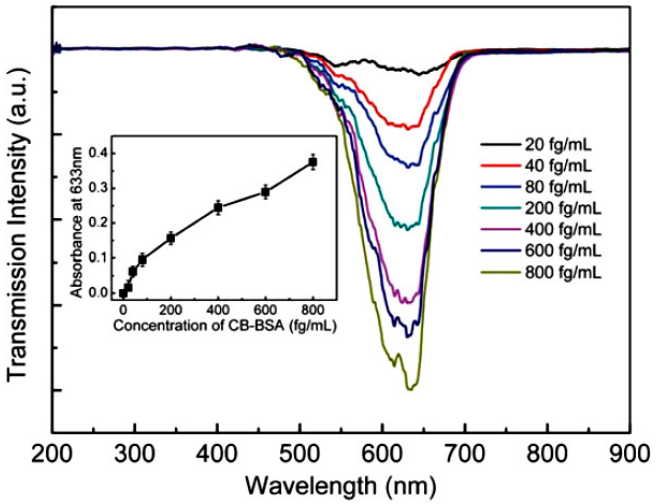


**Figure 1** Measured change in optical transmission through 900 nm waist diameter tapered fiber with changing concentration of Coomassie blue stained bovine serum albumin in a fluidic microchannel. Reprinted with permission from [16]. Copyright 2011, The Royal Society of Chemistry.

### B. Optical fiber sensors for label-free detection in microchannels

Immunoassays generally use labelling with chromophores to create a measurable optical signal, with fluorescent labels the most widely applied method as these offer a high signal to noise ratio [20]. However, the growth and harvesting of the antibodies can take place over weeks and months, and the end products can be relatively expensive. Hence the preparation for, and the undertaking of, an assay, should aim to minimize the number of steps used since each process has a yield and involves wastage of molecules. In addition, the initial tagging process is time consuming and laborious, and the labels themselves can be expensive. Conjugating a label onto a molecule can also hinder the binding or other interaction kinetics during the assay by altering the natural characteristics of the molecule, and this may limit the range of molecules that can be studied or the accuracy of the results obtained.

An alternative to labelling is to develop sensing techniques that can detect binding events without a fluorescent marker. Such a "label-free" sensing approach would allow untagged biological reactions to occur more naturally [21]. An additional motivation to pursue a label-free sensor is that it lends itself to a single step assay, which is a more convenient format for disposable point-of-care platforms with a single wash step from an on-chip fluidic reservoir.

Tian et al. [22] reported an interferometer based on a tapered optical fiber for label-free sensing. For a non-adiabatic taper topology, the tapering region can support more than one optical mode which recombine interferometrically. Any phase changes whilst traversing the tapered region will result in a shift of the interference fringes at the output of the sensor. In a demonstration, the fiber taper was functionalized with IgG antibody and the capture of antigens induced a fringe shift on the output of the sensor. However, this interferometric sensing format required the use of spectral analysis and thus the use of expensive bulk sources and detectors.

A simpler format was reported by Hsu et al. [23] based on optical absorbance. This absorbance derived from a plasmonic resonance between the light and oscillating electrons in a metal nanoparticle deposited on the fiber. The sensor was initially characterized within the microchannel of a microfluidic chip and then applied to real clinical samples from hospital patients. This particular fiber was a plastic-clad silica optical fiber and thus no tapering was required to access the evanescent field giving a significantly greater robustness to general handling. The fiber was simply unclad over a 2 cm mid-section and then coated with a monolayer of nanoparticles functionalized with bioreceptors and then inserted into a microfluidic chip (Figure 2). Because simple absorbance measurements were possible, the optical source consisted of a low-cost light emitting diode (LED) and a photodiode detector. This simple low-cost system showed an estimated sensitivity of $2.9\times10^{-5}$ RIU (refractive index units), whilst the same sensor tested in a conventional macro liquid cell (volume 3 mL) gave a lower sensitivity of $7.0\times10^{-5}$ RIU. The geometry of the microchannel (free volume 14 µL) had increased the sensitivity of the sensor by 2.4-times. The response time of the developed sensor was also enhanced 9-times by the microchannel environment. In addition, long- term testing of these fiber sensors revealed that they could be stored for at least two months and then used without loss of functionality or reproducibility. Finally, the developed sensors were used to detect the levels of MMP-3 in synovial fluid samples from hospitalized patients. The results revealed that the differences between the traditional enzyme-linked immunosorbent assay and the developed fibre optic sensor were regarded as insignificant. Hence, these developed optical fibre sensors were shown to be a viable and successful alternative to established laboratory procedures for use in-situ within microfluidic systems.

More recently, label-free assays mediated by plasmonic resonances allowed Chang et al. [24] to monitor the real-time binding kinetics of both anti-ovalbumin and anti-mouse IgG within a microchannel. Again a low-cost LED and photodiode combination was used with their sensor. They also demonstrated that the sensor could be regenerated for multiple experiments.

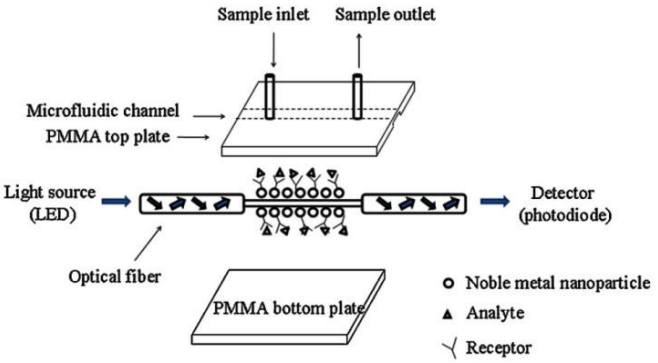


**Figure 2** Optical fiber mid-section coated with metallic nanoparticles and functionalized with receptor molecules to form a biosensor within a microfluidic chip. Reprinted with permission from [23]. Copyright 2011, Elsevier.

## III. OPTICAL FIBER REFRACTOMETERS IN MICROCHANNELS

The measurement of refractive index (refractometry) of a fluid is a common optical measurement with applications in many areas ranging from environmental monitoring [25-27], to manufacturing, e.g. - for determining the composition of liquid mixtures [28], and for applications to biological fluids [29]. Refractive index is often used for protein concentration in blood serum and for urinalysis.

Lei et al. [30] imprinted an optical grating on the end-face of a fiber and positioned this inside a microchannel together with three adjacent light collection fibers. The magnitude of the collected light from each diffracted order varied as the refractive index on the fluid in the microchannel changed, with a detection limit of $4x10^{-4}$ RIU for the zeroth order. Lee et al. [31] showed that the simultaneous measurement of three parameters (temperature, strain, and refractive index) with a tapered fiber Bragg grating sensor could be achieved by detecting the differential response of the guided modes to each parameter. By monitoring the individual Bragg reflections this single sensor within a microchannel could simultaneously detect changes in refractive index to $1x10^{-4}$, changes of strain to 10 microstrain, and temperature changes to 0.32°C accuracy. These results could be further improved (up to ten-times) with additional signal processing.

Chen et al. [32] reported the fabrication of a "multi-D-shaped" optical fiber refractometer sensor within a microchannel. Up to 7 trenches of length 1 mm were micromachined into the side of a multimode fiber (Figure 3). Increasing the number of trenches increases the sensitivity but at the expense of reduced mechanical strength of the sensor. At each trench section the multimode fiber allows multiple internal reflections of the light and thus attenuated total reflection sensing can take place and the light guidance conditions become dependent on the refractive index outside the fiber/medium interface. Using transmitted light intensity measurements a refractive index resolution of $3 \times 10^{-4}$ RIU was achieved within a microchannel. Overall, the sensing approach makes this sensor less complex than an optical fiber grating refractometer. However, the micromachining of an optical fiber requires specialist equipment.

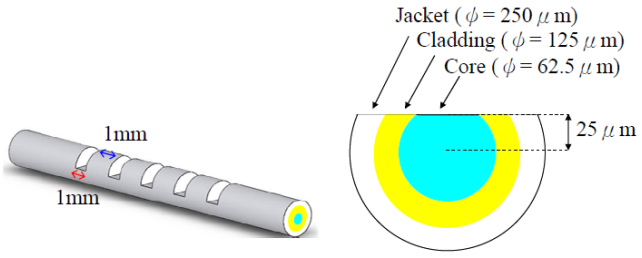


**Figure 3** Schematic showing topology and dimensions of a multimode multi-D-shaped fiber. Reprinted from [32] is permitted for non-commercial purposes. Copyright 2011, MDPI (http://www.mdpi.org).

An optical fiber Farby-Perot cavity refractometer located within a silicon microchannel and demonstrating a particularly low limit of detection of $6 \times 10^{-6}$ RIU was reported by Tian et al. [33]. This level of sensitivity is superior to bulk Abbe refractometers (resolution range between $1x10^{-4}$ to $2x10^{-5}$) [34], and is on a par with the best demonstrated FBG and long period grating refractometers (Table 1). However, these sensors suffer from sensitivity to temperature changes and have the need for spectral analysis. The sensitivity to temperature changes around the developed Farby-Perot sensor was found to be linear at 0.075 nm/°C and could be used for calibration, with a separate sensor in an adjacent microchannel being used solely for temperature sensing. Surface plasmon-based refractometers can have a higher sensitivity (down to $7x10^{-7}$ RIU) but have yet to be demonstrated within fluidic microchannels. Looking ahead, a recent numerical analysis indicated that a surface plasmon-based single-mode fiber refractometer with a bent geometry can achieve a resolution up to $10^{-8}$ RIU [40], which could simply be achieved by bending the microchannel itself.

**Table 1** Example refractive index resolutions achieved with optical fiber refractometers and a traditional Abbe refractometer.

| Optical Fiber Refractometer | Refractive Index Resolution Range |
|---|---|
| Abbe Refractometer [34] | $2x10^{-5}$ |
| Multimode Fiber Interference [35] | $3.3x10^{-5}$ |
| Fiber Bragg Gratings [36] | $2x10^{-6}$ |
| Long Period Gratings [37] | $1.9x10^{-6}$ |
| Optical Fiber Tapers [38] | $3.7 \times 10^{-6}$ |
| Surface Plasmonic Resonance [39] | $7.0 \times 10^{-7}$ |

## IV. OPTICAL FIBER SENSORS FOR IDENTIFYING AND CHARACTERIZING BIO-CHEMICAL MOLECULES IN MICROCHANNELS

In a modern laboratory the optical spectrophotometer is a ubiquitous tool for identification and quantitative measurements on (bio-) chemical molecules within fluids by obtaining optical measurements from ultraviolet to near infrared wavelengths. Such a versatile tool has found regular applications from the physical to the biological sciences and throughout industry, and therefore miniaturized versatile optical spectrometers are an essential requirement for future researchers to reproduce analytical experimentation with a fluidic microchannel. The ability to integrate spectroscopic analysis with the microchannel may also lead to more powerful point-of-care platforms. However, traditional optical components of a spectrometer are bulky and cannot be readily integrated, which somewhat detracts from the advantages and direction of the microfluidic chip technology.

### A. Fiber optic spectroscopy within a microchannel

The closer integration of an optical spectrometer with the microchannel was recently demonstrated by Fan et al. [41] who described a fiber optic probe for the measurement of surface-enhanced Raman scattering (SERS) from molecules within a microchannel. The end of a fiber was functionalized

with five layers of silver nanoparticles using sol-gel as a binding agent (Figure 4). When molecules in a microchannel are illuminated with laser light, a small number of photons can undergo Raman (inelastic) scattering with an excited state vibrational mode of the molecule such that the molecule either gains or loses energy to a re-emitted photon [42]. One advantage of Raman scattering is that molecules having similar chemical composition and whose fluorescence emissions overlap can be individually recognized because the vibrational energies of the molecules will be unique, leading to Raman scattered wavelengths that are distinct and separated. If the molecules are absorbed onto a metal substrate with a surface roughness, an amplification of the Raman signal (SERS) by up to around $10^{10}$ can take place.

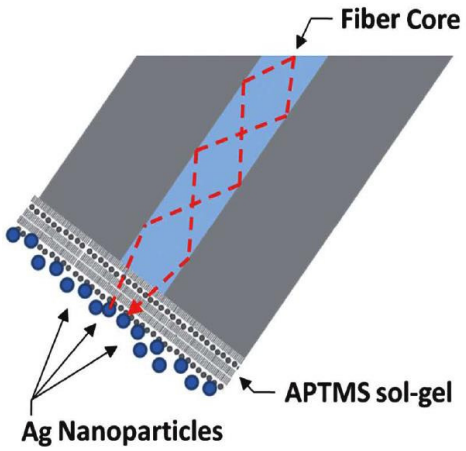


**Figure 4** Fiber end-face functionalized with silver nanoparticles using (3-aminopropyl)trimethoxysilane (APTMS) sol-gel as a binding layer to create a SERS probe for insertion into a microchannel. Reprinted with permission from [41]. Copyright 2012, The Royal Society of Chemistry.

Since the Raman wavelengths are separated from the excitation wavelength, the single fiber probe itself was used to carry both the excitation laser light and collect the SERS signal from the microchannel. Water solutions of five different dyes were individually introduced into the microchannels and the Raman spectra characteristic of each dye could be identified. Subsequently, two solutions containing fluorescent dyes (Nile Blue and Oxazine 170) with overlapping fluorescence emission were mixed at different concentrations and the resultant individual concentration-dependent spectra from the different dye species could easily be distinguished. This sensor has potential for the identification and measurement of individual molecules in a range of bio-chemical applications. In addition, unlike other SERS methods that insert nanoparticles into a microchannel fluid flow and then dispose of those nanoparticles, the optical probe can be cleaned and then re-used.

A long period grating (LPG) optical fiber couples light from the fiber core into cladding modes, and the wavelength selective loss is sensitive to the external refractive index surrounding the fiber cladding without the need to taper the fiber. Wang [43] recently reported the sensing of chloride ions using a LPG integrated into a microfluidic platform. The need for chloride ion measurement in environmental and industrial monitoring, as well as clinical analysis, has led to the employment of traditional methods (titration and colorimetry) and Ion Selective Electrodes (ISEs). Using simple absorbance measurements with a laser diode at 1550 nm, Wang obtained a largely linear change of optical transmission to changing chloride ion concentrations. The performance of the sensor was compared directly with a traditional ISE and demonstrated a very strong correlation ($R^2$ = 0.975) in concentration measurements.

### B. Optical fiber sensor for particle size determination

Fluorescence correlation spectroscopy (FCS) is an established scientific technique that monitors the stochastic fluctuations in fluorescence from a very low number of fluorescent molecules within a small target volume [44]. Within a spherical optical resonator so-called whispering gallery modes (WGMs) can occur when light is totally internally reflected back into the sphere to undergo further reflections [45]. Molecules close to the resonator can change the resonance wavelength, and this technique has been used to detect biomolecules such as proteins [46] and DNA [47]. A spherical resonator in conjunction with a fiber taper was used by Keng et al. [48] in which FCS was extended to non-fluorescent molecules or conversely the optical fiber sensor developed therein could be used for high frequency measurements rather than just a resonance wavelength shift. The evanescent field of a tapered optical fiber was used to establish a WGM around a silica spherical resonator located in a microfluidic channel of a microfluidic cell. It was found that the decay rate of the normalized autocorrelation function was proportional to the inverse diameter of the nanoparticles in the evanescent field of the WGM (Figure 5). This interesting result opens up the possibility of creating new tools for measuring the diameter of species on the scale of nanometres within microfluidic channels.

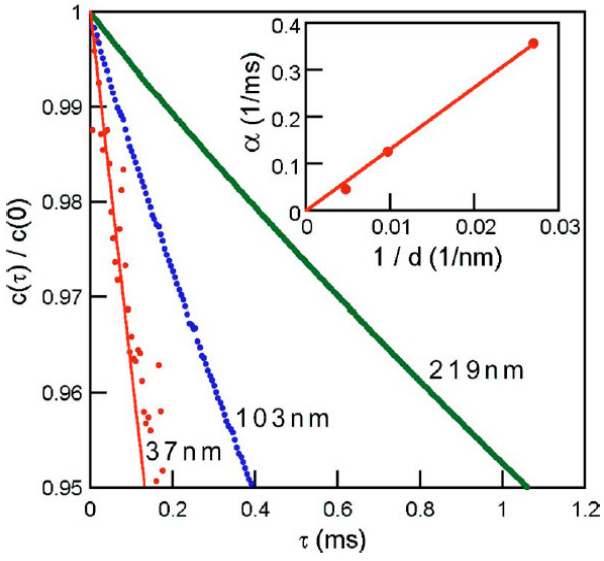


**Figure 5** Decay in average autocorrelation of WGM resonance over 1 msec for nanoparticles with three different diameters. Reprinted with permission from [48]. Copyright 2007, American Institute of Physics).

## V. OPTICAL FIBER SENSORS FOR RHEOLOGY IN MICROCHANNELS

Understanding the motion of the fluid itself within a microchannel is of great importance since at these dimensions liquids do not obey established hydrodynamic laws (e.g. Navier Stokes equations) [49]. Thus miniature sensor devices that can probe microchannels are required to conduct fundamental microflow analysis in real time. Controlling flow on these scales is much harder due to the increased effects of surface roughness on the flow, and small changes of pressure in the macro inlets having amplified effects within the microchannel.

### A. Flow rate sensors in microchannels

Accurate flow rate measurements over a large dynamic range are beneficial in areas such as particles sorting and flow cytometry. Established techniques that have been developed for measuring microchannel flow rates include miniature sensors created by complex MEMS multi-stage processing [50] and particle image velocimetry (PIV) [51] that uses a bulk laser to illuminate tracer particles introduced into the microchannels in conjunction with a microscope-based imaging system.

Lien and Vollmer [52] reported a fiber optic cantilever based flow rate sensor integrated into a microchannel which offered a wider dynamic range, and utilized a less complex architecture than other MEMS-based flow sensors [53]. A 9 µm thick etched single-mode fiber section was suspended transversely across a PDMS microchannel (Figure 6) with the end-face of the fiber aligned in front of a multimode receiving fiber (core diameter 62.5 µm). The reduced single-mode fiber section can still readily guide light if the fluidic refractive index is lower than the original cladding index (approximately 1.463). As fluid flows through the microchannel the mechanical flexibility of the thinned silica fiber section allows it to bend over a large dynamic range of flow rates (0 to 1500 µL/min). This caused the magnitude of optical power transfer between the single-mode fiber and the multimode fiber to be reduced yielding an optical signal proportional to flow. However, the sensor response had both linear and nonlinear components as the flow rate changes due to the non-uniform far-field distribution of the light that is collected by the multimode fiber. This limits the sensor to flow rate ranges that are within the linear region or, alternatively, to employing fibers whose far field profile is more linear, such as dispersion shifted single-mode fibers [54]. In addition, the sensitivity of the sensor can be further improved by increasing the cantilever length and/or reducing the fiber diameter further, but at the expense of overall flow-rate range over which the optical output reaches the multimode fiber.

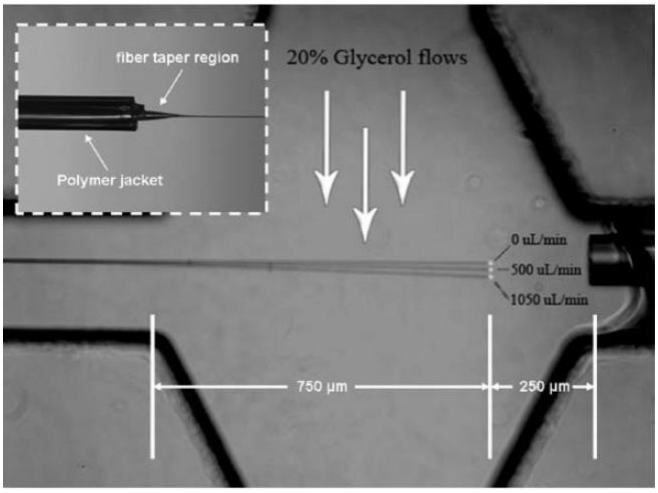


**Figure 6** Flow rate sensor based on a fiber cantilever integrated into a microchannel. Reprinted with permission from [52]. Copyright 2007, The Royal Society of Chemistry.

A different flow rate sensor based on a fiber cantilever that detected both velocity and viscosity of a fluid by using a different analytical technique was reported by Ju et al. [55]. In this case the fiber cantilever was placed parallel to the microchannel axis. For high enough flow rates differential hydrodynamic forces occur around the fiber and results in vibration of the cantilever whose frequency is directly related to both the flow rate of liquid and the liquid viscosity. A fluid flow rate changing from 3 to 15 mL/min could be measured with this experimental setup. This range is very limited when compared to that reported by Lien and Vollmer [52], but this experimental configuration could also be adapted to detect changes in viscosity for a fixed flow rate.

### B. Two-phase flow velocity sensor

Due to their intrinsic large surface-to-volume-ratio a series of microchannels make very efficient heat sinks in a more compact footprint compared to standard cooling methods [56]. Thus, in recent years fluidic microchannels have found increasing use as heat exchangers for cooling components within fuel cells, ever faster microelectronic systems, as microreactors [57, 58] and several other applications [59].

Two-phase fluids (periodic sections of immiscible liquids or liquid and a gas) in microchannels have attracted increasing interest to allow boiling to take place in the channels [60, 61]. Due to the excess heat absorbed when changing from a liquid to a gas (latent heat of vaporization) this enables reduced flow rates within microchannels, as well as the use of less coolant. The flow of individual fluid (immiscible) phases within the same microchannel obey different laws from those in larger classical systems, and thus there is a desire for measurement techniques (preferably non-invasive) that can be applied to study the fluid phases within the microchannel. Currently, bulk imaging techniques are often employed to achieve such measurements [62] but this limits the method to fluidic

structures that are transparent at the measurement wavelength and are usually single layered.

David et al. [63] described an optical fiber sensor format embedded into a microchannel for measuring the size and velocity of droplets in a two phase microflow situation using a "D-shaped" fiber Bragg grating (FBG), where the cladding has been thinned on one side of the fiber so that the evanescent field can be accessed. The average difference in velocity estimations using the fiber sensor and a traditional imaging technique was estimated to be 11.6% and was dependent upon the accuracy of the periodicity and lengths of the FBGs. Therefore with careful control of the fabrication process the fiber optic sensor could be used to replace expensive bulk imaging systems. In addition, the use of fiber optics offers a distributed sensing format and negates the need for special electrical isolation of each sensor.

## VI. Optical Fiber Tools for Manipulation Within a Microchannel

The ability to position an optical fiber within a microchannel gives the opportunity to create a functional tool to actively manipulate flow and materials present in the microchannel rather than just sensing their presence and concentrations.

### A. Fluidic flow control in a microchannel

Vapor bubbles generated in microfluidic systems are often used as micro-actuators with no mechanical moving parts for the creation of pumps, valves, mixers, as well as droplet generators [64]. Pulsed-laser-induced bubble generation is often achieved directly in liquids by adding a dye to increase optical absorption, with the resultant contamination of the fluid and the subsequent requirement to filter the dye from the fluid. Low-power CW lasers have been used to heat metal films to nucleate bubble formation, but optical power loss through the optical path and exposure of fluid samples and biological species to this laser light are drawbacks to this technique. Kim et al. [65] reported a microheater for bubble generation directly within a fluid microchannel using a titanium film coated upon the end of an optical fiber. Depositing the metal on the fiber tool removed the requirement of this metallization fabrication step onto the microchannel system itself, which has been the traditional method used. In addition having the metal film on the end of a fiber removes the need for focusing and aligning a free-space optical system. It was demonstrated by Kim et al. that localized surface plasmons in the metal facilitated heat generation and vapor bubble formation at a much lower laser threshold. Kim et al. demonstrated a microvalve for management of liquid flow control within the microchannel.

### B. Particle sorting and extraction

Exploring the functionality of biological cell components requires single cell manipulation, thus creating the need for cells to be sorted and trapped. The large sample volumes of traditional cell sorting methods, such as centrifugation, fluorescent activated cell sorting (using pre-stained cells) and magnetic cell sorting (using magnetic bead labelled cells), are being replaced by microliters and nanoliters volumes in microchannels [66, 67]. The separation of biological components such as proteins and DNA, or the isolation of cell types (for example, leukocyte from other blood cells) is a valuable tool for subsequent individual analysis further along the microfluidic system.

The evanescent field of an optical fiber has found applications in particles size separation in dynamic fluid flows in a microchannel. For particles in a fluid that are transparent to the optical wavelength, the circular particle acts like a ball lens and focuses the light on the far side of the particle, and if the fluid is more optically absorptive this causes the temperature of the fluid to rise. The non-uniform heat distribution around the particle causes an unbalanced photophoretic force [68] to be exerted on the particle which results in the particle moving towards the optical fiber evanescent field. For particles within a moving fluid the force exerted on the particle by the fluid is dependent on particle size, as is the photophoretic force on a particle.

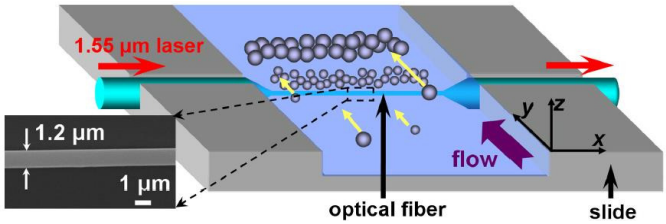


**Figure 7** Tapered optical fiber (inset) perpendicular to fluidic flow used to separate different sized particles within a microchannel. Reprinted with permission from [69]. Copyright 2012, Optical Society of America.

Lei et al. [69] tapered down a mid-section of a single-mode optical fiber to a waist diameter close to 1 μm and suspended this section across a fluidic microchannel (Figure 7). A random suspension of 5 and 10 μm diameter polymer particles were created in fluid flowing into the microchannel. Laser light of wavelength 1550 nm and power 120 mW was launched into the fiber for a period of 30 seconds causing nearby particles to move towards the fiber and distribute themselves roughly according to size. By increasing the fluid flow velocity from 4.5 to 8 μm/s the fluid flow exerts a greater force on the larger particles and a more complete separation of particles by size can be achieved (Figure 8). The technique has also been applied to the removal of microbes from water as a means of purification [70] with a 99.9% removal efficiency. This new fiber optic tool provides a method to add functionality to microfluidic and lab-on-a-chip situations for aggregating and separating cells, and the removal of unwanted material. However, this fiber tool configuration required the application of a high laser power.

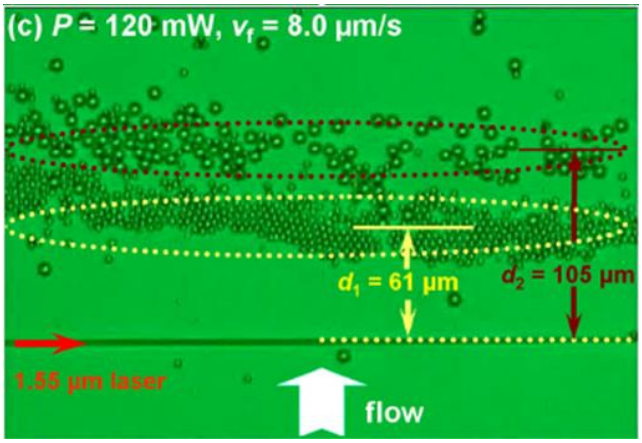


**Figure 8** A random suspension of 5 and 10 µm PMMA particles in water in the vicinity of a tapered optical fiber are separated in size. Reprinted with permission from [69]. Copyright 2012, Optical Society of America.

A different optically induced force (the gradient force) was used by Li et al. [71] to extract particles from a fluid using a sub-micron (700 nm) fiber with deliberate defects (Figure 9 inset) created on the fiber surface by moving it in and out of a flame. The fiber was integrated into a 200 µm microchannel (Figure 9) and a suspension of 3 µm and 700 nm diameter polystyrene particles in water was introduced into the channel. At each defect on the fiber there will be an optically induced gradient force estimated to be three times stronger than that produced at the smooth fiber surface. This represents a trapping force for particles dependent on their size, with the 3 µm diameter particles being trapped more easily. Experiments revealed that with a combination of laser power of only 0.6 mW and a fluid flow rate of 10 µm/s, a high extraction efficiency of 92% for the 3 µm particles could be achieved.

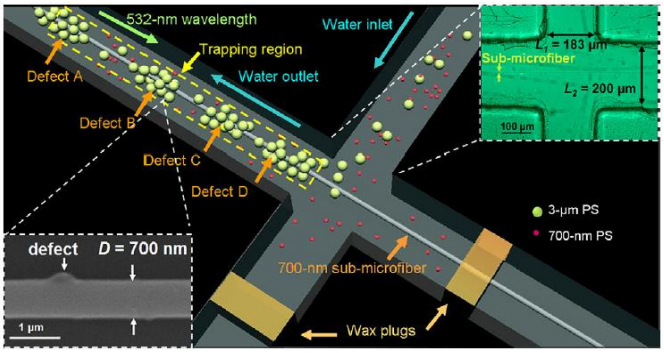


**Figure 9** Particles extraction by size from fluid flow within a microfluidic channel using optical trapping by a submicron fiber with defects (lower inset) created on the fiber surface. Reprinted with permission from [71]. Copyright 2012, American Institute of Physics.

Table 2 contrasts some various methods and optical powers used to sort particles and biological elements within fluidic environments.

**Table 2** Comparison of optical powers used in particle sorting methods

| Particle Sorting Format | Typical Optical Power Levels Required (mW) |
|---|---|
| Waveguide Evanescent Field [72-74] | 35 to 5000 |
| Diode-Bar Optical Trapping [75, 76] | 450 to 2000 |
| Flow Cytometry [77] | 15 to 200 |
| Tapered Micron Fiber [69] | 120 |
| Sub-Micron Fiber with Point Defects [71] | 0.6 |

## C. In-situ trapping with single-ended optical fibers

From their inception in the 1980s, optical tweezers have been used for contactless trapping, manipulation, and fundamental analysis of the full range of biological elements, unveiling the molecular interactions in complex systems like proteins, DNA, cell membranes. The trapping by optical tweezers for manipulating live cells and other biological species in labs is increasing globally, and therefore, a natural progression is optical trapping being applied to microfluidic systems. This would allow, for example, the sorting and trapping of living cells in the fluidic flow and then applying spectroscopic analysis to them, or investigating the metabolism of individual microorganisms [78].

Optical tweezers have traditionally been implemented by focusing laser light through a microscope objective to concentrate the electric field gradient in a localized region. Biological material is pulled towards the location where the electric field reaches a maximum and is held there. Optical tweezers have advantages that the forces generated on the target element are in the piconewtons range thus minimizing damage to the biological material. However, the implementation of optical tweezers through microscope objectives requires bulk optical equipment, careful alignment, produces a restricted field of view, and the sharply focused light within the microchannel elevates the optical power and the risk of damage to the trapped biological species. Hence alternative techniques for the integration of microfluidic systems and optical trapping are being sought.

Trapping of the widely-used bacteria E. coli by traditional optical trapping methods is difficult due its low refractive index contrast to the surrounding aqueous media, and the active swimming of the bacteria. This is exacerbated for the variable flow conditions found in microfluidic platforms. Xin et al. [79] reported how an optical fiber taper positioned at the intersection of four microfluidic channels which was used to trap and manipulate E. coli subjected to variable flow conditions. A wavelength of 980 nm was chosen as it is weakly absorbing by the living cells, but stable trapping could be achieved with a low optical power of 10 mW.

Liberale et al. [80] reported innovative optical tweezers in the form of a custom-made bundle of four optical fibers for insertion into a microfluidic channel. The total diameter of the bundle was 320 µm. At the distal end of each of the four optical fibers a 25 µm high microprism (Figure 10) was formed by photolithography. The geometry and location of each microprism allows the collection of over 95% of the optical power transmitted by each optical fiber. The individual microprisms are designed to redirect (by total internal

reflection) the output light from each fiber towards the center of the fiber bundle. At the point where the four beams cross over, the optical intensity is at a maximum and thus creates an optical trap. The optical trapping distance was designed to be 40 to 55 μm from the fiber end-face to allow flexibility of use in the microchannel platforms. As a demonstration of the capabilities of these novel optical fiber based tweezers, the fiber bundle was inserted through a 360 μm hole created in the base of a 60 μm deep microchannel of a microfluidic chip. With the optical power set at just 5 mW at each microprism, the optical tweezers could easily and stably trap different biological material, such as tumor and red blood cells (Figure 11).

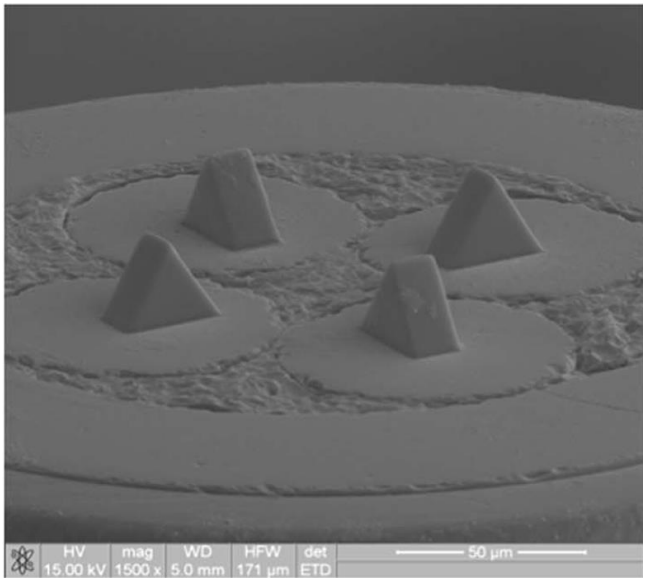


**Figure 10** Microprisms (25 μm high) formed by two-photon lithography on the end-face of individual optical fibers for the creation of optical tweezers. Reprinted with permission from [80]. Copyright 2013, Nature Publishing Group.

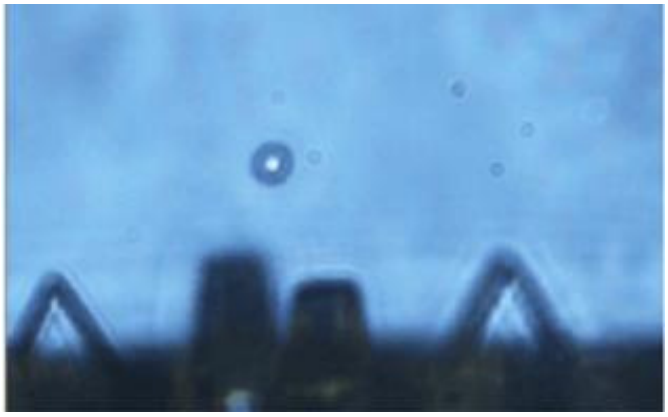

**Figure 11** Image of red blood cell trapped within a microfluidic channel using novel fiber tweezers. Reprinted with permission from [80]. Copyright 2013, Nature Publishing Group.

Fluorescence spectroscopy was demonstrated with the trapping of fluorescent polystyrene beads. Only two microprisms were employed to trap a bead, whilst another prism deflected 532 nm excitation light onto the bead and a conventional microscope lens collected the emitted fluorescence at 640 nm. Similarly, Raman signatures could be recorded from trapped live cells in the microchannel. This innovative fiber optic platform is a significant step forward in the miniaturization of complex optical trapping tools and demonstrates the key role that optical fibers can play. However, the present configuration still requires the employment of a microscope lens to collect generated fluorescence. It is easy to imagine though that a future invasive optical trapping tool could easily incorporate an additional lensed fiber in the center to collect fluorescence signals.

Table 3 compares the power levels required for the optical methods that have been implemented to form optical tweezers for the trapping of particles and biological elements.

**Table 3** Comparison of optical powers levels required in several optical tweezers configurations

| Optical Tweezers Format | Typical Optical Power Levels Required (mW) |
|---|---|
| Holographic Optical Tweezers [81, 82] | 100 to 1000 |
| Conventional Optical Tweezers [83] | 5 to 100 |
| Single-ended Fiber Bundle [80] | 20 |
| Tapered Optical Fiber [79] | 10 |

## VII. Conclusion

Although a relatively small number of optical fiber devices have been demonstrated operating inside microchannels, the variety and inventiveness of the sensors and tools that have been achieved using the fiber optic/microfluidic platform combination is impressive and growing. The fiber geometry lends itself to micron dimensions and, unlike microelectronic devices, the fiber optic can operate within electrically conducting fluids (such as water) without encapsulation and the basic material of the optical fiber platform (silica) is chemically inert.

The versatility of the optical fiber platform has already allowed researchers to conduct immunoassays in microchannels using both fluorescently-labelled and label-free formats whilst gaining advantages of reduced assay time and increased sensitivity. As well as standard measurements, such as refractive index and absorption spectroscopy, more intricate measurements like Raman and fluorescence correlation spectroscopy in the microchannel have also been demonstrated. In addition, fiber optic devices for trapping and sorting biological material give researchers additional tools to conduct traditional experiments directly within a microchannel.

As the scientific world moves inexorably to smaller dimensions, and “nano” becomes the new “micro”, then new flexible nanofiber sensors could come into their own for ultrasensitive detection of single events. The emerging concept of “lab-on-fiber” will give the optical fiber platform additional (highly integrated) functionalities and is already demonstrating novel higher performance devices that can be applied to the fluidic microchannel. Bioengineering on the scale of nanometers will require new tools to manipulate and assemble components, and fiber optic tools may also offer

solutions in this area. With continued miniaturization of photonic devices, simple discrete optical fiber based devices could eventually be replaced by a range of spatial, wavelength or time division multiplexed optical fiber systems incorporated into complex fluidic microsystems.

The potential of fiber optical sensors to make a real impact in the microfluidic world is clear, but nevertheless, the principal stumbling block to greater utility (as with many optical fiber sensors) is that these devices are often individual examples requiring many steps to fabrication and remain far from the stage of mass production that would allow a researcher in the biological sciences to take a sensor off-the-shelf and incorporate it into their microfluidic systems. In the meantime, innovative fiber optic devices for microfluidics continue to be developed and reported.

**Author biographies** Please see Supporting Information online.

## REFERENCES


[1] V. R. Horowitz, D. D. Awschalom, and S. Pennathur, Lab on a Chip **8**, 1856-1863 (2008).

[2] E. Delamarche, D. Juncker, and Heinz Schmid, Adv. Mater. **17**, 2911-2933 (2005).

[3] D. Mark, S. Haeberle, G. Roth, F. von Stetten, and R. Zengerle, Chem. Soc. Rev. **39**, 1153-1182 (2010).

[4] D. Erickson and D. Li, Analytica Chimica Acta **507**, 11-26 (2004).

[5] M. Tanyeri, R. Perron, and I. M. Kennedy, Opt. Lett. **32**, 2529-2531 (2007).

[6] D. Schafer, E. A. Gibson, E. A. Salim, A. E. Palmer, R. Jimenez, and J. Squier, Opt. Express **17**, 6068-6073 (2009).

[7] B. Lincoln, S. Schinkinger, K. Travis, F. Wottawah, S. Ebert, F. Sauer, and J. Guck, Biomed Microdevices **9**, 703-710 (2007).

[8] P. C. Ashok, G. P. Singh, H. A. Rendall, T. F. Krauss, and K. Dholakia, Lab on a Chip **11**, 1262-1270 (2011).

[9] B. Byrne, E. Stack, N. Gilmartin, and R. O'Kennedy, Sensors **9**, 4407-4445 (2009).

[10] K. Eyer, S. Stratz, P. Kuhn, S. K. Küster, and P. S. Dittrich, Anal. Chem. **85**, 3280-3287 (2013).

[11] W. G. Lee, Y.G. Kim, B. G. Chung, U. Demirci, and A. Khademhosseini, Adv. Drug Deliver. Rev. **62**, 449-457 (2010).

[12] D. Hill, B. McDonnell, S. Hearty, L. B. Desmonts, R. Blue, M. Trnavsky, C.McAtamney, R. O'Kennedy, and B. D. MacCraith, Biomed. Microdevices **13**, 759-767 (2011).

[13] D. Hill, S. Hearty, L. B.Desmonts, R. Blue, C. McAtamney, R. O'Kennedy, and B. MacCraith, NSTI NanoTech, Boston June 1-5, **3**, 237-240 (2008).

[14] A. Dudus, R. Blue, and D. Uttamchandani, IEEE Sensors J. **13**, 1594-1601 (2013).

[15] J. Kai, Z. Zou, J.Han, S. H. Lee, B. Hong, Y. Ren, K. A. Kang, and C. H. Ahn, Solid-State Sensors, Actuators and Microsystems, 2007, The 14th International Conference on. pp. 735-738.

[16] L. Zhang, P. Wang, Y. Xiao, H. Yu, and L.Tong, Lab on a Chip **11**, 3720-3724 (2011).

[17] G. Brambilla, J. Opt. **12**, 043001 (2010).

[18] D. J. Sirbuly, A. Tao, M. Law, R. Fan, and P. Yang, Adv. Mater. **19**, 61-66 (2007).

[19] F. Gu, L. Zhang, X. Yin, and L. Tong, Nano Lett. **8**, 2757-2761 (2008).

[20] A. Leung, P. M. Shankar and R. Mutharasan, Sensor. Actuat. B **125**, 688-703 (2007).

[21] S. Ray, G. Mehta and S. Srivastava, Proteomics **10**, 731-748 (2010).

[22] Y. Tian, W. Wang, N. Wu, X. Zou, and X. Wang, Sensors **11**, 3780-3790 (2011).

[23] W. T. Hsu, W. H. Hsieh, S. F. Cheng, C. P. Jen, C. C. Wu, C. H. Li, C. Y. Lee, W. Y. Li, L. K. Chaua, C. Y. Chiang, and S. R. Lyu, Anal. Chim. Acta **697,** 75-82 (2011).

[24] T. C. Chang, C. C. Wu, S. C. Wang, L. K. Chau, and W. H. Hsieh, Anal. Chem. **85**, 245-250 (2013).

[25] Y. V. Mishchenko, Meas. Tech. **50**, 629-637 (2007).

[26] T. L. Bergman, F. P. Incropera, and W. H. Stevenson, Rev. Sci. Instrum. **56**, 291-296 (1985).

[27] A. Banerjee, S. Mukherjee, R. K. Verma, B. Jana, T. K. Khand, M. Chakroborty, R. Das, S. Biswas, A. Saxena, V. Singh, R. M. Hallen, R. S. Rajput, P. Tewari, S. Kumar, V. Saxena, A. K. Ghosh, J. John, and P. Gupta-Bhaya, Sens. Actuat. B **123**, 594-605 (2007).

[28] J. Turan, E. F. Carome, and C. Ovsenik, TELSIKS, **2**, 489-492 (2001).

[29] S. A. Gonchukov, Yu. B. Lazarev, and A. A. Podkolzin, Instrum. Exper. Tech. **43**, 826-828 (2000).

[30] L. Lei,1 H. Li, J. Shi, and Y. Chen, Rev. Sci. Instrum. **81**, 023103 (2010).

[31] S. M. Lee, M. Y. Jeong, and S. S. Saini, J. Lightwave Technol. **30**, 1025-1031 (2012).

[32] C. H. Chen, T. C. Tsao, J. L. Tang, and W. T. Wu, Sensors **10**, 4794-4804 (2010).

[33] Y. Tian, W. Wang, N. Wu, X. Zou, C. Guthy, and X.Wang, Sensors **11**, 1078-1087 (2011).

[34] C. B. Kim and C. B Su, Meas. Sci. Technol. **15**, 1683-1686 (2004).

[35] Q. Wang and G. Farrell, Opt. Lett. **31**, 317-319 (2006).

[36] C. A.J. Gouveia, Refractometric Optical Fiber Platforms for Label Free Sensing, in Current Developments in Optical Fiber Technology, 1st ed. (InTech, 2013) pp.345-372.

[37] T. D. P. Allsop, R. Reeves, D. J. Webb, I. Bennion and R. Neal, Rev. Sci. Instrum., **73**, 1702-1705 (2002).

[38] G. Salceda-Delgado, D. Monzon-Hernandez, A. Martinez-Rios, G. A. Cardenas-Sevilla, and J. Villatoro, Opt. Lett., **37**, 1974-1976 (2012).

[39] D. M. Hernández and J. Villatoro, Sens. Actuators B, **115**, 227-231 (2006).

[40] Y. N. Kulchin, O. B. Vitrik, and A. V. Dyshlyuk, Pac. Sci. Rev., **16**, 73-77 (2014).

[41] M. Fan, P. Wang, C. Escobedo, D. Sinton, and A. G. Brolo, Lab on a Chip **12**, 1554-1560 (2012).

[42] A. Otto, I. Mrozek, H. Grabhorn, and W. Akemann , J. Phys.: Condens. Matter **4**, 1143-1212 (1992).

[43] J. N. Wang, Sensors **11**, 8550-8568 (2011).

[44] M. A. Medina and P. Schwille, BioEssays **24**, 758-764 (2002).

[45] R. Blue, L. Li, G. M H Flockhart, and D.Uttamchandani, J. Micromech. Microeng. **21**, 115020 (2011).

[46] A. M. Armani, R. P. Kulkarni, S. E. Fraser, R. C. Flagan, and K. J. Vahala, Science **317**, 783 (2007).

[47] F. Vollmer, S. Arnold, D. Braun, I. Teraoka, and A. Libchaber, Biophys. J. **85**, 1974 (2003).

[48] D. Keng, S. R. McAnanama, I. Teraoka, and S. Arnold, Appl. Phys. Lett. **91**, 103902 (2007).

[49] G. Hetsroni, A. Mosyak, E. Pogrebnyak, and L.P. Yarin, Int. J. Heat Mass Tran. **48** 1982-1998 (2005).

[50] S. Wu, Q. Lin, Y. Yuen, and Yu-Chong Tai, Sens. Actuat. **A89**, 152-158 (2001).

[51] J. G. Santiago, S. T. Wereley, C. D. Meinhart, D. J. Beebe, and R. J. Adrian, Exp. Fluids **25**, 316-319 (1998).

[52] V. Lien and F. Vollmer, Lab on a Chip **7**, 1352-1356 (2007).

[53] C.-M. Ho and Y.-C. Tai, Annu. Rev. Fluid Mech. **30**, 579-612 (1998).

[54] M. V. Grekov, S.A. Vasil'ev, I. G. Korolev, A. S. Boshkov, O. I. Medvedkov and A. K. Senatorov, Instrum. Exp. Tech. **48**, 96-101 (2005).

[55] P. Y. Ju, C. H. Tsai, L. M. Fu, and C. H. Lin, Solid-State Sensors, Actuators and Microsystems Conference (Transducers), June 5-9, 2011, China, pp. 1428-1431.

[56] D. B. Tuckerman and R. F. W. Pease, IEEE Electr. Device Lett. **EDL-2**, 126-129 (1981).

[57] M. Mohammadi and K. V. Sharp, J. Fluid Eng. **135**, 021202-1 (2013).

[58] P. Abbyad, R. Dangla, A. Alexandrou, and C. N. Baroud, Lab on a Chip **11**, 813-821 (2011).

[59] H. A. Mohammed, G. Bhaskaran, N. H. Shuaib, and R. Saidur, Renew. Sust. Energ. Rev. **15**, 1502-1512 (2011).

[60] W. Qu and I. Mudawar, Int. J. Heat Mass Tran. **46**, 2755-2771 (2003).
[61] J. R. Thome, Int. J. Heat Fluid Fl. **25**, 128-139 (2004).
[62] V. Dore, D. Tsaoulidis, and P. Angeli, Applications of Laser Techniques to Fluid Mechanics, Lisbon, Portugal, 09-12 July, 16th Int Symp on. (2012), pp. 1-12.
[63] N. David, N. Djilali, and P. Wild, Microfluid Nanofluid **13**, 99-106 (2012).
[64] E. Zwaan, S. L. Gac, K. Tsuji, and C-D. Ohl, Phys. Rev. Lett. **98**, 254501-4 (2007).
[65] H-T. Kim, H. Bae, Z. Zhang, A. Kusimo, and M. Yu, Biomicrofluidics **8**, 054126-10 (2014).
[66] P. Chen, X. Feng, W. Du, and B. F. Liu, Front. Biosci. **13**, 2464-2483 (2008).
[67] X. Wang, S. Chen, M. Kong, Z. Wang, K. D. Costa, R. A. Li, and D. Sun, Lab on a Chip **11**, 3656-3657 (2011).
[68] H. Lei, Y. Zhang, X. Li, and B. Li, Lab on a Chip **11**, 2241-2246 (2011).
[69] H. Lei, Y. Zhang, and B. Li, Opt. Express **20**, 1292-1300 (2012).
[70] Y. Zhang, H. Lei, Y. Li, and B. Li, Lab on a Chip **12**, 1302-1308 (2012).
[71] L. Li, H. Xin, H. Lei, and B. Li, Appl. Phys. Lett. **101**, 074103 (2012).
[72] B. S. Schmidt, A. H. J. Yang, D. Erickson, and M. Lipson, Opt. Express **15**, 14322-14334 (2012).
[73] B. S. Ahluwalia, P. McCourt, T. Huser, and O. G. Hellesø, Opt. Express **18**, 21053-21061 (2010).
[74] S. Kawata and T. Tani, Opt. Lett. **21**, 1768-1770 (1996).
[75] R. W. Applegate Jr., J. Squier, T. Vestad, J. Oakey, D. W. M. Marr, P. Bado, M. A. Dugan, and A. A. Said, Lab on a Chip **6**, 422-426 (2006).
[76] R. A. Applegate, Jr., J. Squier, T. Vestad, J. Oakey, and D. W. M. Marr, Appl. Phys. Lett. **92**, 013904-3 (2008).
[77] J. Picot, C. L. Guerin, C. Le Van Kim, and C. M. Boulanger, Cytotechnology **64**, 109-130 (2012).
[78] B. Landenberger, H. Hofemann, S. Wadle, and A. Rohrbach, Lab Chip, **12**, 3177-3183 (2012).
[79] H. Xin, Y. Li, L. Li, R. Xu, and B. Li, Appl. Phys. Lett. **103**, 033703-4 (2013).
[80] C. Liberale, G. Cojoc, F. Bragheri, P. Minzioni, G. Perozziello, R. La Rocca, L. Ferrara, V. Rajamanickam, E. Di Fabrizio, and I. Cristiani, Sci. Rep. **3**, 1258 (2013).
[81] J. E. Curtis, B. A. Koss, and D. G. Grier, Opt. Commun. **207**, 169-175 (2002).
[82] W. J. Hossack, E. Theofanidou, and J. Crain, Opt. Express **11**, 2053-2059 (2003).
[83] K. C. Neuman and S. M. Block, Rev. Sci. Instrum. **75**, 2787-2809 (2004).